

# High frequency photoacoustic imaging for *in vivo* visualizing blood flow of zebrafish heart

Jinhyoung Park,<sup>1</sup> Thomas M. Cummins,<sup>1</sup> Michael Harrison,<sup>2</sup> Jungwoo Lee,<sup>4</sup> Qifa Zhou,<sup>1,\*</sup> Ching-Ling Lien,<sup>2,3</sup> and K. Kirk Shung<sup>1</sup>

<sup>1</sup>NIH Resource on Medical Ultrasonic Transducer Technology, Department of Biomedical Engineering, University of Southern California, Los Angeles, CA 90089, USA

<sup>2</sup>Saban Research Institute, Children's Hospital Los Angeles, Los Angeles, CA 90027, USA

<sup>3</sup>Department of Surgery, University of Southern California, Los Angeles, CA 90033, USA

<sup>4</sup>Department of Electronic Engineering, Kwangwoon University, Seoul, South Korea

\*qifazhou@usc.edu

**Abstract:** A technique on high frame rate(28fps), high frequency co-registered ultrasound and photoacoustic imaging for visualizing zebrafish heart blood flow was demonstrated. This approach was achieved with a 40MHz light weight(0.38g) ring-type transducer, serving as the ultrasound transmitter and receiver, to allow an optic fiber, coupled with a 532nm laser, to be inserted into the hole. From the wire target study, axial resolutions of 38 $\mu$ m and 42 $\mu$ m were obtained for ultrasound and photoacoustic imaging, respectively. Carbon nanotubes were utilized as contrast agents to increase the flow signal level by 20dB in phantom studies, and zebrafish heart blood flow was successfully observed.

©2013 Optical Society of America

OCIS codes: (110.0110) Imaging systems; (110.5120) Photoacoustic imaging.

---

## References and links

1. K. D. Poss, L. G. Wilson, and M. T. Keating, "Heart regeneration in Zebrafish," *Science* **298**(5601), 2188–2190 (2002).
2. J. R. Hove, "In vivo biofluid dynamic imaging in the developing Zebrafish," *Birth Defects Res. C Embryo Today* **72**(3 Part C), 277–289 (2004).
3. J. Park, Y. Huang, R. Chen, J. Lee, T. M. Cummins, Q. Zhou, C. L. Lien, and K. K. Shung, "Pulse Inversion Chirp Coded Tissue Harmonic Imaging (PI-CTHI) of zebrafish heart using high frame rate ultrasound biomicroscopy," *Ann. Biomed. Eng.* **41**(1), 41–52 (2013).
4. L. Sun, X. Xu, W. D. Richard, C. Feng, J. A. Johnson, and K. K. Shung, "A high-frame rate duplex ultrasound biomicroscopy for small animal imaging in vivo," *IEEE Trans. Biomed. Eng.* **55**(8), 2039–2049 (2008).
5. J. M. Yang, C. Favazza, R. Chen, J. Yao, X. Cai, K. Maslov, Q. Zhou, K. K. Shung, and L. V. Wang, "Simultaneous functional photoacoustic and ultrasonic endoscopy of internal organs in vivo," *Nat. Med.* **18**(8), 1297–1302 (2012).
6. T. Harrison, J. C. Ranasinghesagara, H. Lu, K. Mathewson, A. Walsh, and R. J. Zemp, "Combined photoacoustic and ultrasound biomicroscopy," *Opt. Express* **17**(24), 22041–22046 (2009).
7. Y. Zhang, H. Hong, and W. Cai, "Photoacoustic imaging," *Cold Spring Harb Protoc* **2011**(9), 1015–1025 (2011).
8. J. Park, C. Hu, and K. K. Shung, "Stand-alone front-end system for high-frequency, high-frame-rate coded excitation ultrasonic imaging," *IEEE Trans. Ultrason. Ferroelectr. Freq. Control* **58**(12), 2620–2630 (2011).
9. J. M. Cannata, T. A. Ritter, W. H. Chen, R. H. Silverman, and K. K. Shung, "Design of efficient, broadband single-element (20-80 MHz) ultrasonic transducers for medical imaging applications," *IEEE Trans. Ultrason. Ferroelectr. Freq. Control* **50**(11), 1548–1557 (2003).
10. E. K. Pugach, P. Li, R. White, and L. Zon, "Retro-orbital injection in adult zebrafish," *J. Vis. Exp.* **34**(34), 1645 (2009).

---

## 1. Introduction

The zebrafish heart is well known for its regenerative capability [1]. The heart can fully recover resected tissue after amputation of up to 20% of the ventricle. Conventional histology studies require sacrificing the fish to investigate the damaged heart making further follow up with the same fish impossible. As a non-invasive method, optical cameras have been employed to identify both tissue and blood flow regeneration in embryonic zebrafish because of the embryos' transparent nature [2]. For adult zebrafish, high frequency (>40 MHz) ultrasound techniques have been employed for observing the morphological changes in clots

formed in the amputated sites [3]. However the intracardiac blood flow, which can be a key indicator of functional recovery, has not been visualized at high resolution or only in a confined region with the use of pulsed Doppler imaging methods [4].

In order to visualize the live zebrafish heart, an imaging system capable of high pulse repetition rate ( $> 50$  fps) and high spatial resolution ( $< 40 \mu\text{m}$ ) is required [4]. Blood flow may be conventionally visualized via high frequency ultrasound power Doppler imaging. Due to transmitted signals of multi-cycled burst with an array imaging system, this may require high frequency transmission over 70 MHz to reach the required fine spatiotemporal resolution. However, a high frequency array system at such a high frequency has not been introduced. The other applicable method for detecting blood flow with ultrasound is photoacoustic imaging that can achieve better contrast resolution than that of ultrasound by using a pulsed laser for transmission instead of a sound burst. Recently, a photoacoustic system integrated into an endoscope was employed to derive three dimensional images of blood vessels in the rabbit esophagus that were hardly identifiable with ultrasound images alone [5]. High frequency ( $> 25$  MHz) photoacoustic tomography (PAT) was also built to visualize blood flow in a human finger [6]. In this case, co-registered ultrasound-photoacoustic imaging method helped identifying blood vessels which could not be found otherwise. However, high frame rate photoacoustic imaging could not be achieved yet because of either low scanning speed or the limited pulse repetition rate of the typical laser systems.

In this paper, a technique for detecting the blood flow of live zebrafish heart is reported. The technique was implemented in a photoacoustic scanning system that included a 40 MHz light weight transducer. Contrast agents made of single wall carbon nano-tubes (SWNT) were utilized to increase the received photoacoustic signals [7]. The transducer's sensitivity was designed to be sufficient enough to allow the detection of the signals produced by the high pulse repetition rate (10 kHz) laser when its output dropped under  $75 \mu\text{J/pulse}$ . Both phantom and in-vivo studies are carried out, and the results are promising to demonstrate the feasibility of photoacoustic imaging in visualizing the blood flow in zebrafish hearts.

## 2. Implementation

### 2.1 System configuration

The system implemented was designed to achieve co-registered ultrasound with photoacoustic imaging. A pulsed laser was combined with a custom designed biomicroscope, capable of high frame rate ( $>68$  fps) and, high frequency ( $< 70$  MHz) operation [8]. Overall system configurations were shown in Fig. 1. While the mechanical sector scanner translated the transducer from the right to the left within the scanning angle of 8 degrees, trigger signals for ultrasound and photoacoustic imaging were alternately sent out to the ultrasound transmitter and the 532 nm pulsed laser (Spectra-Physics Explorer, Newport Corporation, Irvine, CA) respectively in 20 kHz. The speed of the motor was 26 round trips per second, and each image frame having 100 ultrasound and 100 photoacoustic scanlines was acquired on one-way translation. A two cycle sine burst, and a laser pulse were transmitted at ultrasound and photoacoustic trigger time. The triggering sequences are illustrated in Fig. 2. The acoustic signals from both imaging modalities were digitized by an analog to digital converter (CS14200, GaGe Applied Technologies Inc., Lachine, QC, Canada) and processed/saved by a custom made LabView (LabView 5.0, National Instruments, Austin, TX) based software program. Co-registration of the acquired ultrasound and photoacoustic signals were processed using the saved RF data in MATLAB. A photoacoustic beamline and its adjacent ultrasound beamline on the right were approximated to be from the same location for co-registrations producing 100 scanlines out of 200 beamlines per one frame.

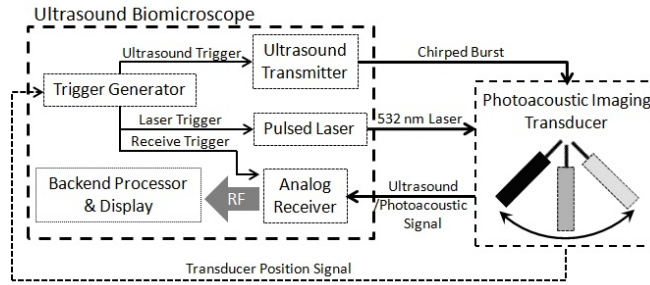


Fig. 1. Block diagram of custom designed high frame rate imaging system capable of co-registered high frequency ultrasound and photoacoustic imaging. The trigger signal generator takes position signal and distributes trigger signals for acquiring photoacoustic and ultrasound signals simultaneously.

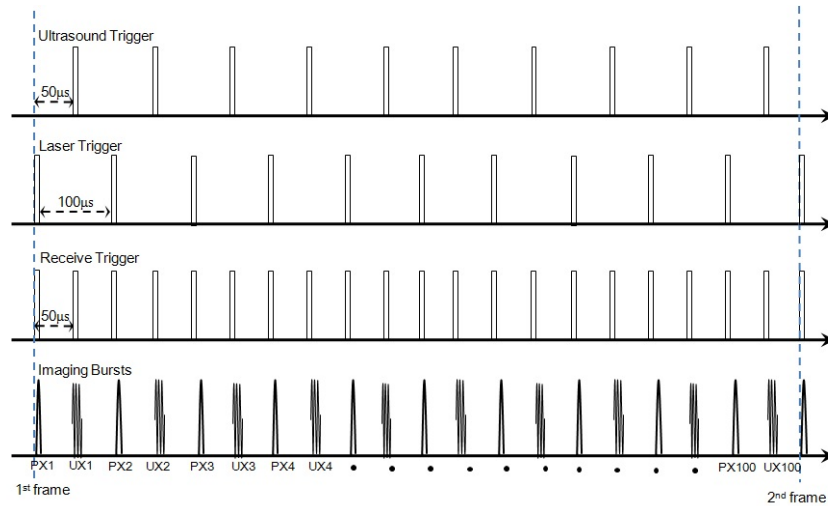


Fig. 2. Beam sequences for the co-registered imaging. From the top row, trigger signals for transmitting ultrasound and laser and receiving echo signals for analog to digital converter are shown. In the last row, the alternating photoacoustic (PX) and ultrasound transmits (UX) are depicted.

## 2.2 Light weight photoacoustic transducer

A single element lithium niobate ( $\text{LiNbO}_3$ ) confocal transducer was designed to be light weight (0.38 g) so it could perform high frame rate ( $>26$  fps) ultrasound and photoacoustic imaging. The acoustic stack was comprised of four layers, backing,  $\text{LiNbO}_3$  and two matching layers. The housing was fabricated out of titanium to minimize weight and was turned down to a cylinder with an inner diameter 3.5 mm, outer diameter 3.9 mm and a height of 7.6 mm. The acoustic stack was then fixed inside the metal housing using Epotek-301 epoxy (EPO-TEK, Billerica, Massachusetts). The detailed fabrication process was described in a previous report [9]. A 0.6 mm hole was then drilled in the center of the transducer to allow a polyimide tube to be inserted and aligned with the ring-shaped transducer. The transducer face was press-focused to achieve a geometric focus at 6 mm using a stainless steel ball with a 6 mm radius to force the transducer face into a curved shape. The polyimide tube (Inner diameter: 0.45 mm, outer diameter: 0.6 mm) was inserted into the hole to guide optic fiber placement. The other side of the tube was pulled out from the transducer housing through the upper edge as shown in Fig. 3 and fixed with Epotek-301 epoxy (EPO-TEK, Billerica, Massachusetts). A multi-mode optic fiber (BFH22-200, ThorLABS, Newton, NJ)

having 0.4 mm of diameter was then inserted through the polyimide tube, and the amount of insertion can be manually adjusted to put the optic fiber's tip close to the imaging target to obtain high level of photoacoustic signal from the zebrafish heart with a small amount of laser energy ( $< 75 \mu\text{J}/\text{pulse}$ ). From the pulse-echo measurement shown in Fig. 3, the center frequency, the peak frequency and the bandwidth were 36 MHz, 40 MHz and 83% respectively

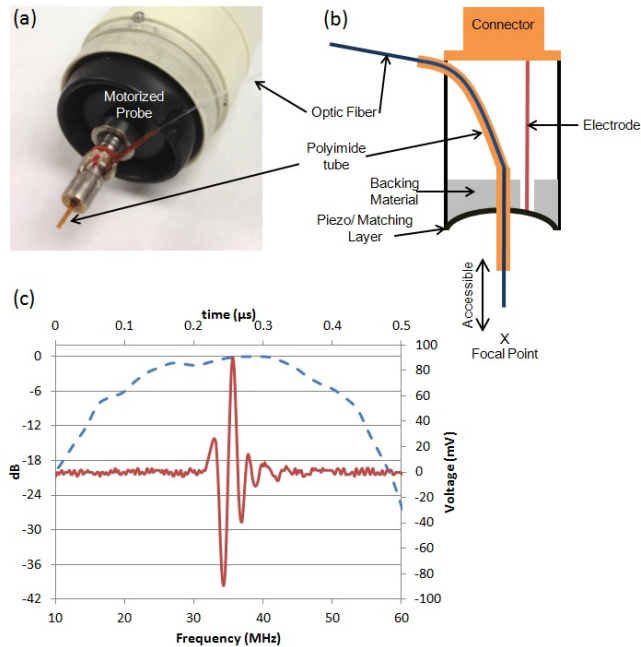


Fig. 3. (a) Picture and (b) mechanical design of the implemented light weight photoacoustic imaging transducer. (c) Pulse echo test result shown in time (solid line) and frequency (dotted line) domains.

### 3. Experimental Setup

#### 2.1 Contrast Agent

NH<sub>2</sub> functionalized single wall carbon nano-tubes (SWNTs) were prepared as a contrast agent to visualize the blood flow in a zebrafish heart. Note that NH<sub>2</sub> radical is chosen to make the SWNT soluble and to be a potential targeted agent for the future purpose. SWNTs (sku-0103, chiptubes.com, Brattleboro, VT) having outer diameter of 1-2 nm and length of 0.5-2  $\mu\text{m}$  were mixed with de-ionized water, and the weight density became 0.06 w/w%. The agent was then sonicated in a sonic bath (57X, Ney Dental International, CT, USA) for an hour to make SWNT solution.

#### 2.1 Phantom Study

In order to evaluate the performance of the photoacoustic imaging system, a 5  $\mu\text{m}$  tungsten wire target and flow phantom were prepared. The wire target was immersed in the de-ionized water and placed at the focal distance of the transducer (6 mm), and the optic fiber tip was pulled out to 4.5 mm from the transducer surface. The flow phantom was a polyimide tube (Inner diameter: 700  $\mu\text{m}$ ) placed at 6 mm within de-ionized water, and one side of the tube was connected with a syringe pump to produce either de-ionized water or SWNT solution flow. The cross-sectional views of both the wire targets and the tubes were acquired with the co-registered ultrasound and photoacoustic imaging.

## 2.1 In-Vivo Study

Adult Zebrafish were anesthetized in a 0.1% tricaine solution (MS-222, Ethyl 3-aminobenzoate methanesulfonate salt, Sigma-Aldrich, St. Louis, MO). Anesthetized fish were placed on a damp sponge under a dissecting scope and 10 $\mu$ l of SWNT solution was injected either retro-orbitally or directly into the sinus venosus. Retro-orbital injection was carried out using a Hamilton syringe as described in a previous study [10]. For sinus venosus injections a 1-1.5mm incision was made with surgical scissors caudally from the chest bone and the heart was exposed with tweezers. Contrast agent was then injected dorsally of the atrium using a pulled glass capillary fitted to a mouth pipette. Photoacoustic imaging was carried out on exposed hearts with a 1-1.5mm diameter plastic ring inserted to hold the chest wall open. Fish were submerged in water containing 0.1% tricaine and placed under the submerged photoacoustic probe for imaging. The optic fiber tip was then adjusted to be as close as possible to the fish heart.

## 4. Results

Figure 4 shows the wire phantom results. Ultrasound and photoacoustic imaging are shown in Figs. 4(a)-4(b), and their axial and lateral brightness profiles are presented in Figs. 4(c)-4(d) respectively. The axial and the lateral resolutions are 38  $\mu$ m and 70  $\mu$ m, respectively for ultrasound, and 42  $\mu$ m and 70  $\mu$ m, respectively for photoacoustic imaging. Note that the error less than 3  $\mu$ m in measuring axial resolution could be made due to the limited sampling rate of 200 MHz. An echo signal to noise ratio of 40 dB can be achieved with photoacoustic imaging.

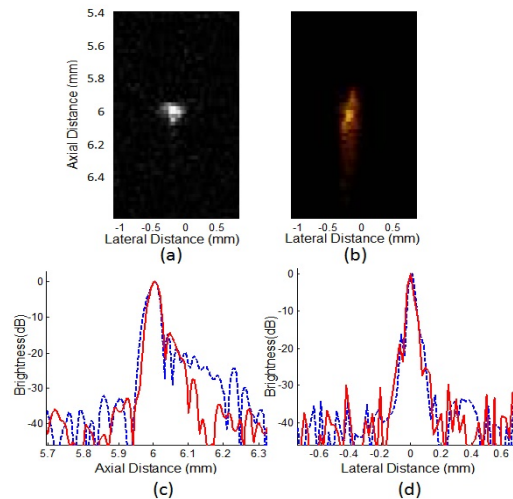


Fig. 4. Wire phantom study results. Images acquired by (a) ultrasound, (b) photoacoustic method. (c) Axial brightness profiles and (d) lateral brightness profiles are provided. Note that red solid line and blue dashed line indicate ultrasound and photoacoustic profiles respectively.

Figure 5 shows cross-sectional views of the flow phantom with the co-registered ultrasound and photoacoustic images. Ultrasound and photoacoustic signals are separated with the different color maps, gray and red respectively. When the tube is filled with deionized water in Fig. 5(a), the photoacoustic signal from the tube center is hardly identifiable. In contrast, following injection of SWNT solution the photoacoustic signal increased by 20 dB within the tube. Here the brightness was measured with an image analysis program (ImageJ 1.44p, National Institutes of Health, USA). Consequently, it is shown that the SWNT solution is capable of generating an increased photoacoustic signal within flows allowing the blood stream to be visualized.

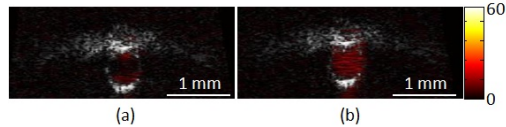


Fig. 5. Coregistered ultrasound images (gray scale) with photoacoustic images (red scales). Images show cross sectional view of a plastic tube filled with (a) pure de-ionized water or (b) de-ionized water with carbon nano particles. Note that The scale of colorbar is dB.

Figure 6(a) shows a zebrafish heart image with co-registered ultrasound and photoacoustic imaging. By opening the chest, the exposed ventricle can be identified with B-mode. The flowing blood within the heart can be identified with photoacoustic imaging with SWNTs, but not with photoacoustic imaging only in Fig. 6(b). Dotted arrows indicate flow streams from atrium to ventricle, which can be identified in the movie file at 26 fps. Underneath the skin where weak laser pulse energy can reach, small blood vessels are visualized, and tissue artifacts within the liver and gills are also identified as a less dynamic signal than the blood flow signal shown in the provided movie. Figure 6(c) shows the same frame of Fig. 6(a), but the static tissue signals are more suppressed by subtracting the RF signals of the previous frame from the ones of the current frame.

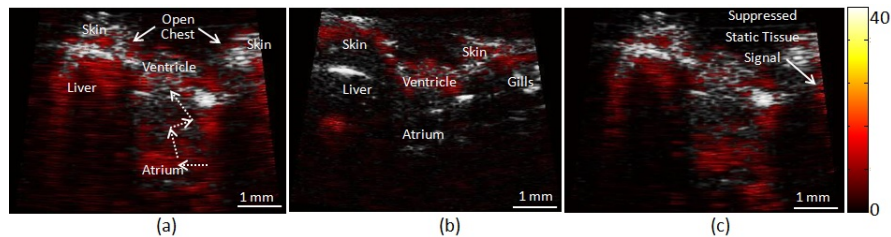


Fig. 6. Zebrafish heart co-registered ultrasound images (gray scale) with photoacoustic images (red scale) (a) with and (b) without SWNT contrast agent and (c) shows the co-registered image with contrast agent and static tissue signal suppression. Dotted arrows indicate blood flow found in the provided movie ([Media 1](#)). Note that the scale of colorbar is dB.

## 5. Discussion and Conclusion

Previously, the frame rate of high frequency photoacoustic imaging has been limited to a rate less than 10 fps because the laser burst energy drops significantly with the increase of pulse repetition rate despite the frame rate of B-mode being higher than 30 fps. With this limitation, fast moving objects cannot be adequately visualized with the photoacoustic imaging. In this current study, three novel approaches, namely, adjustable optical fiber position relative to a target, the use of contrast agent and the light weight ring transducer, allow the increase of photoacoustic image acquisition rate to 26 fps and pulse repetition rate of 10 kHz. Potentially a frame rate of 56 fps could be achieved without compromising with the current image quality by using two-way scanning methods. Although the blood stream in the fish heart was visualized, the signal strength was not as high as the signal level shown in the flow phantom study. Not every injected SWNT will be delivered to the heart because of the long SWNT (2  $\mu\text{m}$ ) compared to the diameter of microvessel in the delivery path and its relative final concentration in the systemic blood will be lower than that of the phantom study. With further optimization of the contrast agent for zebrafish hearts it may be possible to increase the observed signal level. Also, the frame subtraction approach shown in Fig. 6(c) works on suppressing the static tissue signal, but still showing leakages due to the low frame rate causing the decorrelations between the tissue signal of each frame. The increase of frame rate by two-way scan might help more suppressing the static signals than the current one-way scan method.

In conclusion, an imaging system capable of acquiring co-registered high frequency ultrasound and photoacoustic image at a high frame rate is developed. The results show from

the phantom studies that the spatial resolution and signal to noise ratio of photoacoustic imaging was similar to B-mode imaging, and the photoacoustic signal from the flowing blood mixed with SWNTs could be acquired. With these techniques, the blood flowing in the zebrafish heart could be visualized for the first time to the best of our knowledge, and this approach may be used for studying functional recovery of zebrafish heart following injuries.

### **Acknowledgments**

This work has been supported by NIH grants R01-HL79976 and P41-EB2182 and by CIRM training grant TG2-01168 and the research grant of Kwangwoon University in 2012.